An Algebraic Framework for Digital Envelope Modulation

Simon Bicaïs, Jean-Baptiste Doré
CEA-Leti, Minatec Campus, Grenoble, France
contact: simon.bicais@cea.fr

***Abstract*—Sub-THz communications based on coherent receivers suffer from strong phase impairments issued by oscillators. Envelope detection, inherently robust to this impairment, is hence considered for the design of sub-THz systems. This paper proposes an algebraic framework for envelope modulation. In the first place, we introduce a Hilbert space to represent waveforms with non-negative real values. This space is defined by transport of structure of the usual signal-space $\mathcal{L}^2$. So, existing schemes developed for real-valued signals can be exploited upon envelope modulation. In the second place, it is shown that the proposed framework provides powerful tools to design new envelope modulation schemes. To do so, we present the transmission of an In-phase Quadrature signal upon an envelope modulation to prevent the impact of phase noise on communication performance. We also demonstrate that constraints on embedded analog-to-digital converters can be relaxed with the use of orthogonal non-negative waveforms.**

***Index Terms*—Sub-THz communications, Amplitude modulation, Envelope detectors, Linear algebra, Hilbert space.**

I. Introduction

Context & motivations: Wireless communications within the *sub-THz* spectrum (100-300 GHz) are contemplated to face the exponential data traffic growth [1]. The sub-THz spectrum offers unprecedentedly large bands, yet it involves severe radio-frequency impairments that must be mitigated. In particular, sub-THz communications suffer from strong phase impairments issued by oscillators: phase noise, carrier frequency offset [2]. Researches have either addressed compensation of phase impairments [3] or signal processing optimization [4] [5] to enable the development of coherent sub-THz systems. In contrast, non-coherent schemes have long been exploited, *e.g.* On-Off Keying (OOK) at 260 GHz in 2012 [6], for they achieve robustness with low complexity. Indeed, envelope detection is inherently robust to phase impairments. It is hence a valuable scheme to perform frequency translation within sub-THz receivers. Subsequently, it is relevant to consider the design of sub-THz communications systems based on envelope modulation and detection.

Literature: Signal-spaces $\mathcal{L}^2$ and ℓ^2 are usually used for communication design [7]. They provide powerful analytical tools for real and complex valued signals and have lead to the design of performant systems. Though they are not particularly well-suited to describe non-negative signals, these spaces have also been exploited to develop envelope modulation schemes. For instance, the digital modulation techniques used in visible light communications exploit non-negative waveforms: *e.g.* OOK, Pulse Position Modulation (PPM), *etc* [8]. To the best of our knowledge, the development of an algebraic framework dedicated to digital envelope modulation has not been addressed by the literature. This prompts us to define an appropriate Hilbert space for non-negative real valued waveforms in order to enable the design of efficient envelope modulation schemes adapted to sub-THz communications.

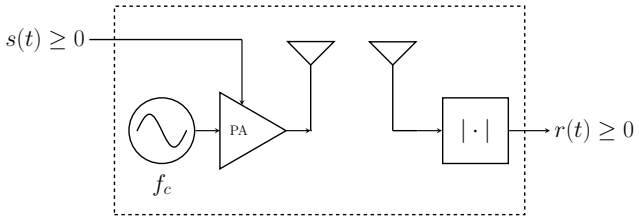

Fig. 1: Frequency translation performed with envelope modulation and detection.

Contributions: In this paper, we propose an algebraic framework for envelope modulation. In the first place, we introduce a Hilbert space to represent waveforms with non-negative real values. This enables to redefine fundamental properties and operators for non-negative signals: orthogonality, projection, *etc*. Nonetheless, we also desire to exploit existing schemes developed for real signals. Therefore, the introduced Hilbert space is defined by transport of structure of signal-space $\mathcal{L}^2$. In the second place, we show that the proposed framework provides efficient tools to design envelope modulation schemes. We hence study the transmission of an In-phase Quadrature (IQ) signal upon an envelope modulation to prevent the impact of phase noise on communication performance. Further, it is demonstrated that constraints on embedded Analog-to-Digital Converters (ADC) may be relaxed with the use of orthogonal non-negative waveforms.

Organization: The paper is organized as follows. The system model is described in Sec. II. We introduce in Sec. III the algebraic framework for envelope modulation. Sec. IV presents potential applications of the proposed framework to sub-THz communications. Eventually, Sec. V concludes the paper.

II. System Model

A. Communication system

Sub-THz systems based on coherent receivers suffer from severe phase impairments issued by oscillators [2]. Envelope detection is thus relevant to perform frequency translation without phase impairments. In addition, envelope modulation allows an efficient use of power amplifiers [9]. For these reasons, we consider a communication system based on envelope modulation and detection as depicted in Fig. 1. At the transmitter, the band-limited modulating signal is denoted s and lies in $\mathbb{R}_{\geq 0} = \{s(t) \in \mathbb{R},\ s(t) \geq 0\}$. The transmitted signal at carrier frequency f_c is then expressed by

$$s_{f_c}(t) = s(t)\cos(2\pi f_c t + \phi(t)), \tag{1}$$

978-9-0827-9703-9/19/$31.00 ©2019 IEEE

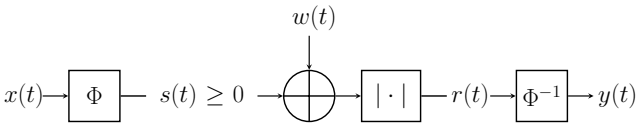

Fig. 2: Illustration of the non-negative channel.

where ϕ represents the oscillator phase noise. At the receiver, the down frequency translation is realized by an envelope detector. Typically, envelope detectors rely on a self-mixer combined with a low-pass filter. First, multiplying the signal by itself yields

$$s_{f_c}(t)^2 = s(t)^2 \cdot \frac{1+\cos(4\pi f_c t + 2\phi(t))}{2}. \tag{2}$$

Then, it is sufficient to filer images at $2f_c$ and take the square root in order to recover the signal of interest s. The details on the implementation of envelope detectors exceed the scope of this study though. It is hence assumed that the detector perfectly demodulates the envelope s of the received signal s_{f_c}.

B. Channel

It has been recently confirmed by measurement campaigns [10] that the line-of-sight component prevails in sub-THz channels. We hence study a waveform corrupted by an Additive White Gaussian Noise (AWGN). The channel is assumed to be equalized and the receiver synchronized. The received signal is given by

$$r(t) = |s(t) + w(t)|\,,\ t \in \mathbb{R}, \tag{3}$$

where w is a zero-mean real Gaussian process with spectral density $2\sigma_w^2$. The noise w is filtered at the input of the envelope detector and is hence band-limited. Hereafter, we will refer to Eq. (3) as the Non-Negative Channel (NNC). It also meaningful to introduce the discrete-time model of the NNC where the received symbol at instant k is expressed by

$$r_k = |s_k + w_k|\,,\ k \in \mathbb{N}, \tag{4}$$

where s_k is the k-th positive real-valued symbol modulated with duration T and $w_k \sim \mathcal{N}(0, \sigma_w^2/T)$.

III. Algebraic Framework

A. Stakes

Hilbert spaces provide an efficient framework for the development of communication systems. Linear signal analysis, processing and reconstruction are entirely developed upon the properties of Hilbert spaces. For instance, optimal filtering exploits the concept of orthogonality, meanwhile the projection theorem is used in approximation problems. Nonetheless, conventional algebraic structures are primarily designed for real-valued signals and are not well-suited to envelope modulation. By means of example, it is difficult for a set of non-negative signals to be orthogonal with the usual inner product of real functions. A common set of orthogonal signals with non-negative values is the set of pulses with different positions in time. This set is exploited in the PPM but requires a precise synchronization between the transmitter and the receiver. In contrast, we intend in this work to define an algebraic framework that could enable the design of new envelope modulation schemes adapted to sub-THz communications. To do so, non-negative waveforms, whose values lies in $\mathbb{R}_{\geq 0}$, are represented within a Hilbert space. This space is denoted H_ρ for continuous waveforms and h_ρ for discrete signals. Moreover, we also desire to exploit the signal processing techniques developed for real-valued signals. Therefore, the Hilbert space H_ρ is defined by *transport of structure* of the signal-space $\mathcal{L}^2$ – or ℓ^2 in the discrete case. The transport of structure $\Phi : \mathcal{L}^2 \to H_\rho$ relies on a bicontinuous function Φ in order to bond real-valued waveforms to non-negative ones. The use of map Φ in the NNC is depicted in Fig. 2. Here and subsequently, we write $\mathcal{L}^2$ the Hilbert space $\left(\mathcal{L}^2([0,T]), \langle\cdot,\cdot\rangle\right)$, the set of square-integrable functions with domain $[0,T]$ equipped with $\langle\cdot,\cdot\rangle$ the usual inner product of real functions. Similarly, ℓ^2 denotes the Hilbert space of square-summable sequence. We first present the transport of structure of Hilbert spaces and then detail the definition of H_ρ.

B. Transport of structure and Hilbert spaces

1) From vector space V_1 to V_2: We first consider two sets S_1, S_2 and a homeomorphism $\Phi : S_1 \to S_2$. Further, the set S_1 equipped with vector addition $+$ and scalar multiplication $\times$ over the field F defines a vector space $V_1 = (S_1, +, \times)$. We next study $V_2 = (S_2, \oplus, \otimes)$ the set S_2 equipped with the vector addition $\oplus$ and the scalar multiplication $\otimes$ over field F defined as follows. Set $u_1, v_1 \in V_1$ and $\lambda \in F$. We denote $u_2 = \Phi(u_1), v_2 = \Phi(v_1) \in V_2$, then the vector addition is defined by

$$u_2 \oplus v_2 = \Phi\left(\Phi^{-1}(u_2) + \Phi^{-1}(v_2)\right) = \Phi(u_1 + v_1), \tag{5}$$

and the scalar multiplication by

$$\lambda \otimes u_2 = \Phi\left(\lambda \times \Phi^{-1}(u_2)\right) = \Phi(\lambda \times u_1). \tag{6}$$

Proposition 1. *$V_2 = (S_2, \oplus, \otimes)$ is a vector space over the field F.*

Proof: Proposition 1 is easily proven by showing that V_2 satisfies the eight axioms of a vector space. □

2) From Hilbert space H_1 to H_2: Let the inner product $\langle\cdot,\cdot\rangle_1 : V_1 \times V_1 \to F$ such that $H_1 = (V_1, \langle\cdot,\cdot\rangle_1)$ is a Hilbert space. Subsequently, the set S_1 is a complete metric space when equipped with the distance induced from the inner product $d_1(u_1, v_1) = \sqrt{\langle u_1 - v_1, u_1 - v_1\rangle_1}$. We next evaluate $H_2 = (V_2, \langle\cdot,\cdot\rangle_2)$, where the map $\langle\cdot,\cdot\rangle_2 : V_2 \times V_2 \to F$ is defined by

$$\langle u_2, v_2\rangle_2 = \langle \Phi^{-1}(u_2), \Phi^{-1}(v_2)\rangle_1 = \langle u_1, v_1\rangle_1. \tag{7}$$

Proposition 2. *$H_2 = (V_2, \langle\cdot,\cdot\rangle_2)$ is an inner product space.*

Proof: Proposition 2 is easily proven by showing that H_2 satisfies the three axioms of an inner product space. □

It is worth mentioning that H_2 defines a norm $\|\cdot\|_2$ and a metric $d_2(\cdot,\cdot)$ upon its inner product expressed by:

$$\|u_2\|_2 = \sqrt{\langle u_2, u_2\rangle_2}, \tag{8}$$

$$d_2(u_2, v_2) = \sqrt{\langle u_2 \oplus \neg v_2, u_2 \oplus \neg v_2\rangle_2}, \tag{9}$$

where $\neg v_2$ stands for the opposite of vector v_2.

Proposition 3. *$H_2 = (V_2, \langle\cdot,\cdot\rangle_2)$ is a Hilbert space.*

Proof: To prove that $H_2 = (V_2, \langle\cdot,\cdot\rangle_2)$ is a Hilbert space, it is sufficient to show that (S_2, d_2) is a complete metric space since $(V_2, \langle\cdot,\cdot\rangle_2)$ is already proved to be an inner product space. To do so, we exploit the property that (S_2, d_2) and (S_1, d_1) are isometric. Isometry preserves completeness - more precisely, uniformly continuous function maps Cauchy sequences into Cauchy sequences - and (S_1, d_1) is known to be complete. It follows immediately that (S_2, d_2) is a complete metric space. □

3) Properties of transport of structure: Such definition of H_2 upon H_1 is referred to as a transport of structure whose properties are listed below.

Theorem 1. *Let the transport of structure $\Phi : H_1 \to H_2$, then the following properties are sastified:*

1) *Φ is surjective and preserves the inner product.*
2) *Φ is surjective and isometric.*
3) *Φ maps an orthonormal basis for H_1 into an orthonormal basis for H_2.*

Proof: We first recall that H_2 is defined such that Φ is surjective and preserves the inner product. Therefore, property 1) is satisfied and the other properties follow easily. This theorem may also be demonstrated from the observation that $\Phi : H_1 \to H_2$ is a bounded linear operator by definition of H_2. For a deeper discussion of operators on Hilbert spaces, we refer the reader to [11]. □

C. Definition of envelope Hilbert space H_ρ

We will now use the previously described results on transport of structure of Hilbert spaces to define an algebraic framework for envelope modulation. As aforementioned, we also desire to rely on conventional Hilbert space $\mathcal{L}^2$. Subsequently, we have

$$\begin{aligned} \Phi : \mathcal{L}^2 &\to H_\rho, \\ : x(t) &\mapsto s(t), \end{aligned} \tag{10}$$

where x is a real-valued waveform. To ensure the soundness of envelope modulation, Φ is subject to the following constraint: the image of x must be non-negative *i.e.* $\Phi : x(t) \mapsto s(t) \in \mathbb{R}_{\geq 0}$. As an illustration, an offset may be sufficient to map a real-valued waveform onto the non-negative real space. This could also be achieved with the exp function, for instance. The Hilbert space $H_\rho = (V_\rho, \langle\cdot,\cdot\rangle_\rho)$ is defined by vector space V_ρ and inner product $\langle\cdot,\cdot\rangle_\rho$. The vector space V_ρ denotes the set $\Phi(\mathcal{L}^2([0,T]))$ equipped with vector addition $\oplus$ and scalar multiplication $\otimes$ over the field $\mathbb{R}$ defined by Eq. (5) and (6). Furthermore, the inner product $\langle\cdot,\cdot\rangle_\rho$ on vector space V_ρ is defined from Φ and the usual inner product of real functions $\langle\cdot,\cdot\rangle$ by Eq. (7). It is worth mentioning that Hilbert space H_ρ can be extended to higher dimensions by Cartesian product. It is sufficient to define vector space operations component-wise and to set the inner product as the sum of the inner products associated to the different components. As represented in Fig. 2, the NNC may also be expressed by

$$y(t) = \Phi^{-1}\left(\left|\Phi\big(x(t)\big) + w(t)\right|\right), \tag{11}$$

where x and y are real-valued signals.

In a similar manner to the definition of H_ρ upon $\mathcal{L}^2$ for continuous waveforms, the envelope Hilbert space h_ρ for discrete signals is defined upon ℓ^2. Due to space limitation, this is not detailed here.

D. Orthonormal sequences in H_ρ

Orthonormal sequences play an important role in communication systems to design orthogonal code modulation or multiplexing schemes. We here introduce them in the context of H_ρ. A set $\boldsymbol{\psi} = \{\psi_n\}_{1\leq n\leq N}$ of N vectors in H_ρ is orthonormal if it satisfies $\forall n_1, n_2$, $\langle\psi_{n_1}, \psi_{n_2}\rangle_\rho = \delta_{n_1 n_2}$. Then, the *synthesis operator* refers to the linear isomorphism from $\mathbb{R}^N$ onto H_ρ defined by

$$\varphi : \boldsymbol{\lambda} \mapsto u = \lambda_1 \otimes \psi_1 \oplus \cdots \oplus \lambda_N \otimes \psi_N, \tag{12}$$

where $u \in H_\rho$ and $\boldsymbol{\lambda} = (\lambda_1, \cdots, \lambda_N) \in \mathbb{R}^N$. We may also use the notation $u = (\boldsymbol{\lambda})_{\boldsymbol{\psi}}$ to define a vector u by its coordinates $\boldsymbol{\lambda}$ relatively to $\boldsymbol{\psi}$. Conversely, given a vector $u \in H_\rho$ the *analysis operator* is the inverse map $\varphi^{-1} : H_\rho \to \mathbb{R}^N$ that evaluates coordinates $\boldsymbol{\lambda}$ of u w.r.t. $\boldsymbol{\psi}$. By orthonormality of $\boldsymbol{\psi}$, we have

$$\lambda_n = \langle u, \psi_n\rangle_\rho. \tag{13}$$

Theorem 1 gives that a sequence $\boldsymbol{\psi}$ is orthonormal in H_ρ if and only if the sequence $\bar{\boldsymbol{\psi}} = \Phi^{-1}(\boldsymbol{\psi})$ is orthonormal in $\mathcal{L}^2$. Accordingly, any orthonormal sequence in $\mathcal{L}^2$ can be exploited upon envelope modulation with an appropriate map Φ. In contrast to the aforementioned example on PPM, this result entails that new orthogonal code modulation or multiplexing schemes can be designed with non-negative waveforms.

IV. Applications

The objective of this section is to give the reader some application examples. In particular, it aims to illustrate that the proposed framework enables the design of efficient envelope modulation schemes adapted to sub-THz communications. Subsequently, the focus is neither on the thorough performance evaluation of the described systems nor on the details of their implementations.

A. Transmission of an IQ signal upon envelope modulation

IQ architectures are a predominant implementation for wireless communications. Though it is a mature technology, it is highly sensitive to phase noise. We desire to benefit from this maturity, and still, achieve robustness for sub-THz systems. Therefore, we investigate the transmission of an IQ signal upon an envelope modulation. The considered system is depicted in Fig. 3. The IQ signal is expressed by

$$x(t) = x_I(t)\cos\left(2\pi f_i \cdot t\right) - x_Q(t)\sin\left(2\pi f_i \cdot t\right), \tag{14}$$

with f_i the intermediate frequency. The pulse shaping of quadrature signals x_I and x_Q is performed with rectangular function, *i.e.*

$$\begin{aligned} x_I(t) &= \sum_k x_{I,k} \cdot \Pi(t - kT), \\ x_Q(t) &= \sum_k x_{Q,k} \cdot \Pi(t - kT), \end{aligned} \tag{15}$$

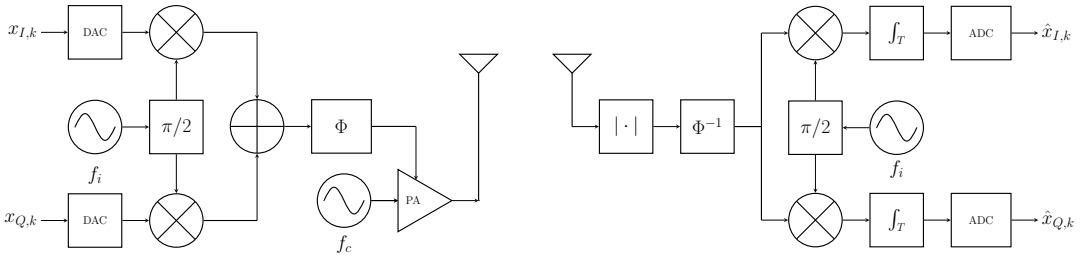

Fig. 3: Transmission of an IQ signal with envelope modulation.

TABLE I: Performance loss in SNR to achieve BER$= 10^{-6}$ induced by the described envelope modulation.

Modulation	4-QAM	16-QAM	64-QAM
ΔSNR(dB)	5.52	6.65	7.48

where $x_{I,k} = \Re(x_k)$, $x_{Q,k} = \Im(x_k)$ and x_k is k-th complex modulated symbol. The signal x is mapped to $s \in H_\rho$ with function Φ. By means of example, we consider

$$\Phi : x(t) \mapsto s(t) = \arctan\left(x(t)\right) + \nu. \tag{16}$$

where ν is the appropriate offset ensuring that s is positive. Signal s modulates the envelope of the transmitted signal[1] around $f_c + f_i$ over the NNC. By Eq. (11), the demodulated signal is expressed by

$$y(t) = \tan\left(r(t) - \nu\right). \tag{17}$$

With regard to the continuity of the $\tan$ function, values of r greater than $\pi/2 + \nu$ must be truncated. Quadrature signals y_I and y_Q are next obtained by projecting y respectively onto $\cos$ and $\sin$. For the in-phase component, that is

$$y_I(t) = \int_T y(t) \cdot \cos\left(2\pi f_i \cdot t\right) dt, \tag{18}$$

Symbols are estimated by sampling these signals every kT time instants:

$$\hat{x}_{I,k} = y_I(kT), \qquad \hat{x}_{Q,k} = y_Q(kT). \tag{19}$$

Table I outlines the performance loss induced by the use of this envelope modulation to transmit an IQ signal. The simulated results presents the difference in Signal-to-Noise Ratio (SNR) to achieve a Bit-Error Rate (BER) of 10^{-6} between the described envelope modulation and a coherent IQ transceiver. Simulations are performed with an IQ signal based on Quadrature-Amplitude-Modulation (QAM) constellations. Though these performance loss may be considered significant, they do not question the relevance of the introduced framework for sub-THz communications. Indeed, sub-THz systems lie in a different paradigm where the critical deterioration is the phase impairments. Besides, it has been shown in [5] that the impact of phase noise on a coherent transmission is not a performance loss in terms of SNR but causes the BER to reach an error floor. In contrast, the presented transmission of an IQ signal over envelope modulation may achieve any targeted BER. Therefore, in comparison to a communication system impacted by phase noise, this scheme appears to be relevant for sub-THz applications. Eventually, these performance losses are only valid for the considered map Φ, unoptimized. We have outlined this specific envelope modulation to illustrate the potential applications of the proposed framework to sub-THz communications, yet some other functions Φ may be designed to achieve better performance.

[1]The image at $f_c - f_i$ can be filtered in order to transmit a single-sideband signal.

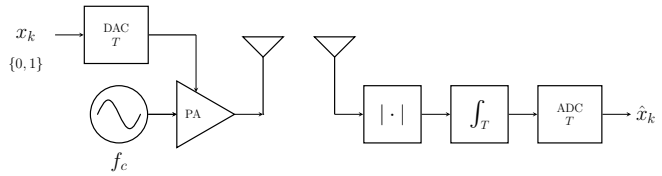

Fig. 4: Illustration of a serial OOK transceiver

B. Relaxing constraints on embedded ADC

One of the contemplated applications for the sub-THz communications is the *kiosk* scenario [12]: A short-range hot-spot supplies users with a high data-rate down-link. Receivers architectures must remain simple in order to be embedded into users' terminals. Even if low complexity schemes are implemented, *e.g.* OOK, it is difficult for embedded ADC to sample several GHz of band. Our objective is therefore to relax the constraints on ADC. We show that the sampling rate of ADC can be made twice slower by multiplexing symbols on two orthogonal non-negative waveforms

Let us first describe a transceiver with a serial architecture as represented in Fig. 4. The studied modulation is an OOK[2]. Symbols $x_k \in \{0, 1\}$ are transmitted on the NNC described in Eq. (3) with a rectangular pulse shaping, *i.e.* $s(t) = \sum_k x_k \cdot \Pi(t - kT)$. The receiver estimates symbols $\hat{x}_k$ by sampling every kT time-instants the signal $r(t) * \Pi(t)$ as illustrated in Fig. 4. In this case, the sampling rate of the ADC is equal to the symbol rate.

Conversely, we now present an architecture where the receiver is parallelized. Modulating symbols $\boldsymbol{x} = (x_{2k}, x_{2k+1}) \in \{0, 1\}^2$ are mapped onto an orthogonal sequence $\boldsymbol{\psi}$ composed of vectors $\boldsymbol{\psi}_1, \boldsymbol{\psi}_2 \in h_\rho^2$. The transmitted symbols $\boldsymbol{s} = (s_{2k}, s_{2k+1})$ are defined by

$$\boldsymbol{s} = (\boldsymbol{x})_{\boldsymbol{\psi}}. \tag{20}$$

By way of illustration, we consider $\boldsymbol{\psi}$ to be the image of Hadamard code $\bar{\boldsymbol{\psi}} = \{(1, 1), (1, -1)\}$ by map $\Phi(x) = x + 1$.

[2]The presented multiplexing may also be exploited with any modulation.

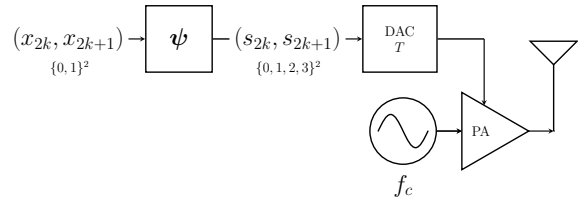

(a) Serial transmitter.

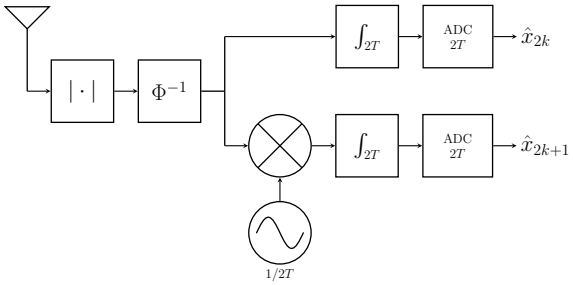

(b) Parallel receiver.

Fig. 5: Illustration of a parallel OOK transceiver.

At the transmitter, mapping from $\boldsymbol{x}$ to $\boldsymbol{s}$ is achieved by the synthesis operator introduced in Eq. (12)

$$\begin{aligned} \boldsymbol{s} &= x_{2k} \otimes \boldsymbol{\psi_1} \oplus x_{2k+1} \otimes \boldsymbol{\psi_2}, \\ &= \Phi(x_{2k} + x_{2k+1}, x_{2k} - x_{2k+1}). \end{aligned} \tag{21}$$

The transmitter keeps a serial architecture, yet it no longer sends $x_k \in \{0,1\}$ but $s_k \in \{0,1,2,3\}$. Incidentally, complexity in the base station is not an issue in the considered scenario. Moreover, it is easier to realize Digital-to-Analog Converters (DAC) with high sampling rates than ADC. At the receiver, symbols may be estimated from the received sequence $\boldsymbol{r}$ by the analysis operator defined in Eq. (13)

$$\hat{x}_{2k} = \langle \boldsymbol{r}, \boldsymbol{\psi_1} \rangle_\rho, \quad \hat{x}_{2k+1} = \langle \boldsymbol{r}, \boldsymbol{\psi_2} \rangle_\rho. \tag{22}$$

Nonetheless, this may also be realized within the continuous time domain since a Hadamard code may actually be regarded as the DFT on the two-element additive group $\mathbb{Z}/(2)$. This requires first to evaluate $y(t) = \Phi^{-1}(r(t))$ and second to project y onto two signals, one constant and the other oscillating with frequency $1/2T$. As depicted in Fig. 5, these projections are expressed by

$$y_1(t) = \int_{2T} y(t) dt, \tag{23}$$

$$y_2(t) = \int_{2T} y(t) \cdot \frac{\pi}{2} \sin\left(\frac{2\pi}{2T} t\right) dt. \tag{24}$$

The receiver finally obtains symbol estimates by sampling these signals every $2kT$ time instants, *i.e.*

$$\hat{x}_{2k} = y_1(2kT), \qquad \hat{x}_{2k+1} = y_2(2kT). \tag{25}$$

This achieves the desired objective. For a fixed symbol rate, the receiver demodulates the symbols based on ADC whose sampling rates are twice slower. Furthermore, this can be easily extended to N orthogonal non-negative waveforms, and thus, to systems with N times slower ADC. Still, it is straightforward to show that the presented multiplexing entails a performance loss in SNR ($\simeq 4.77$ dB). However, this scheme is unoptimized and could be improved. We have presented it in order to illustrate the potential applications of the introduced framework to sub-THz communications.

C. Perspectives

This paper is an introductory work proposing an analytical framework for digital envelope modulation. It should hence be followed by an investigation of performant digital envelope modulation techniques for sub-THz systems. Furthermore, it is worth mentioning that the introduced framework represents a first step in describing analytically polar transceivers [9] where the phase and the amplitude are modulated separately.

V. Conclusion

In this paper we have proposed an algebraic framework for envelope modulation. Non-negative real waveforms have been represented within an appropriate Hilbert space. This space is defined by transport of structure of the usual signal-space $\mathcal{L}^2$ which enables to exploit existing schemes developed for real-valued waveforms upon envelope modulation. It is further shown that the introduced framework may be used to design efficient envelope modulation schemes for sub-THz communications. By way of illustration, we have studied the transmission of an IQ signal with an envelope modulation to prevent the impact of phase noise. We have also demonstrated that the constraints on embedded ADC may be relaxed with the use of orthogonal non-negative waveforms.

References

[1] G. Fettweis, F. Guderian, and S. Krone, "Entering the path towards Terabit/s wireless links," in *2011 Design, Automation Test in Europe*, March 2011, pp. 1–6.

[2] M. Voicu, D. Pepe, and D. Zito, "Performance and Trends in Millimetre-Wave CMOS Oscillators for Emerging Wireless Applications," *International Journal of Microwave Science and Technology*, vol. 2013, p. 6, 2013.

[3] T. Shao, H. Shams, P. M. Anandarajah, M. J. Fice, C. C. Renaud, F. van Dijk, A. J. Seeds, and L. P. Barry, "Phase Noise Investigation of Multicarrier Sub-THz Wireless Transmission System Based on an Injection-Locked Gain-Switched Laser," *IEEE Transactions on Terahertz Science and Technology*, vol. 5, no. 4, pp. 590–597, July 2015.

[4] R. Krishnan, A. G. i Amat, T. Eriksson, and G. Colavolpe, "Constellation optimization in the presence of strong phase noise," *IEEE Transactions on Communications*, vol. 61, no. 12, pp. 5056–5066, December 2013.

[5] S. Bicaïs, J. Doré, and J. G. Jimenez, "On the Optimum Demodulation in the Presence of Gaussian Phase Noise," in *2018 International Conference on Telecommunications (ICT)*, June 2018.

[6] J. Park, S. Kang, S. V. Thyagarajan, E. Alon, and A. M. Niknejad, "A 260 GHz fully integrated CMOS transceiver for wireless chip-to-chip communication," in *2012 Symposium on VLSI Circuits (VLSIC)*, June 2012, pp. 48–49.

[7] J. Proakis, *Digital Communications 5th Edition*, ser. McGraw-Hill series in electrical and computer engineering : communications and signal processing. McGraw-Hill, 2007.

[8] M. S. Islim and H. Haas, "Modulation Techniques for Li-Fi," *ZTE Communications*, vol. 14, pp. 29–40, 04 2016.

[9] J. Groe, "Polar transmitters for wireless communications," *IEEE Communications Magazine*, vol. 45, no. 9, pp. 58–63, September 2007.

[10] L. Pometcu and R. D'Errico, "Characterization of Sub-THz and mmWave Propagation Channel for Indoor Scenarios," in *12th European Association on Antennas and Propagation (EurAAP 18)*, Apr 2018.

[11] K. H. Zhu, "Operator theory in function spaces," 01 1990.

[12] J.-B. Doré, Y. Corre, S. Bicais, J. Palicot, E. Faussurier, D. Kténas, and F. Bader, "Above-90GHz Spectrum and Single-Carrier Waveform as Enablers for Efficient Tbit/s Wireless Communications," in *25th International Conference on Telecommunications (ICT'2018)*, Saint-Malo, France, Jun. 2018.